

Supporting Information for

Dense Arrangement of Crown Ethers in Graphene: Novel Graphitic Carbon Oxides with Enhanced Optoelectronic Properties

HongYan Li^a, Jiang Xiang^a, Liang Chen^{b,a}, Jing Xu^{a,} and Wei Liu^{a,*}*

^a Department of Optical Engineering, College of Optical, Mechanical and Electrical Engineering, Zhejiang A&F University, Hangzhou, Zhejiang, 311300, P. R. China

^b School of Physical Science and Technology, Ningbo University, Ningbo, Zhejiang, 315211, P. R. China

Email: weiliu@zafu.edu.cn; jingxu@zafu.edu.cn.

Keywords: Graphene; Defects; Nanopores; First-principles calculations; Optical adsorption.

Table S1. The nanopore density of CmG-n (m=3-6, n=1-6).

System	C _x O _y	primitive cell area (Å ²)	nanopore density (Å ⁻²)	System	C _x O _y	primitive cell area (Å ²)	nanopore density (Å ⁻²)
C3G-1	C ₄ O ₃	20.22	4.95	C5G-1	C ₂₈ O ₂₀	144.59	2.77
C3G-2	C ₁₂ O ₆	51.24	3.90	C5G-2	C ₁₄ O ₁₀	73.24	2.73
C3G-3	C ₁₆ O ₆	60.59	3.30	C5G-3	C ₂₀ O ₁₀	90.82	2.20
C3G-4	C ₁₆ O ₆	60.72	3.29	C5G-4	C ₁₀ O ₅	45.46	2.20
C3G-5	C ₈ O ₃	30.93	3.23	C5G-5	C ₁₀ O ₅	45.58	2.19
C3G-6	C ₆₈ O ₃	189.21	0.53	C5G-6	C ₆₄ O ₅	188.27	0.53
C4G-1	C ₆ O ₄	28.73	3.48	C6G-1	C ₆ O ₆	39.16	2.55
C4G-2	C ₈ O ₄	35.64	2.81	C6G-2	C ₁₂ O ₆	58.70	1.70
C4G-3	C ₃₆ O ₁₆	146.00	2.74	C6G-3	C ₁₂ O ₆	58.93	1.70
C4G-4	C ₁₈ O ₈	75.13	2.66	C6G-4	C ₁₂ O ₆	59.24	1.69
C4G-5	C ₁₈ O ₈	76.22	2.62	C6G-5	C ₁₄ O ₆	64.70	1.55
C4G-6	C ₆₆ O ₄	188.60	0.53	C6G-6	C ₆₀ O ₆	186.55	0.54

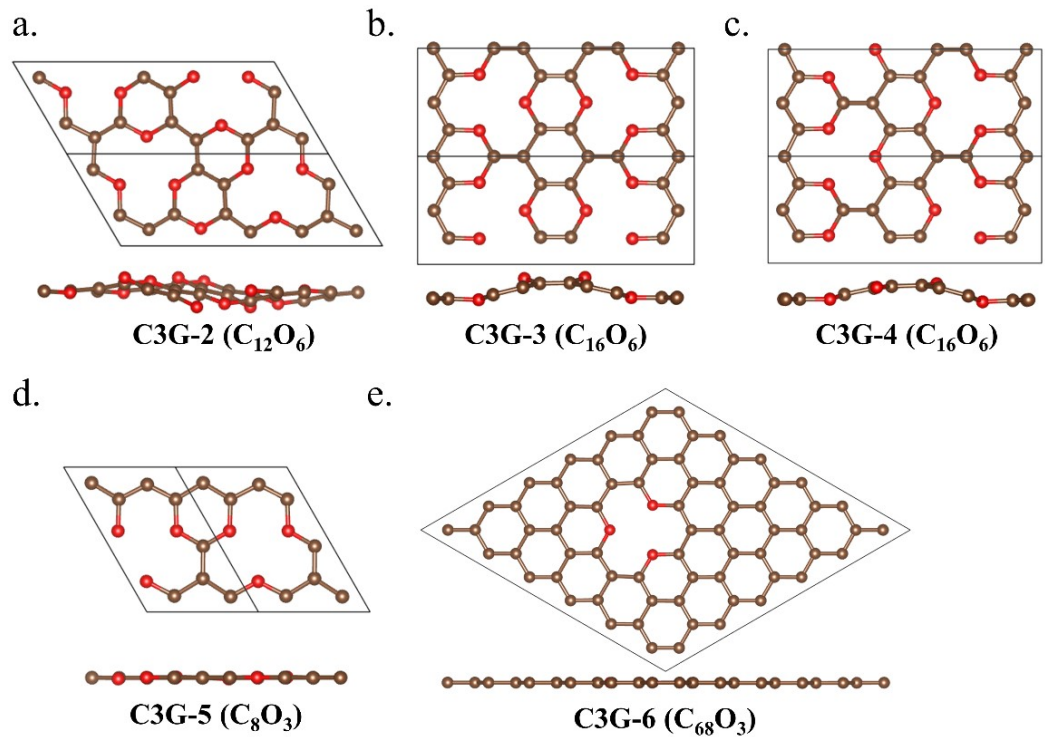


Figure S1. Top and side views of the optimized structures of (a) C3G-2, (b) C3G-3, (c) C3G-4, (d) C3G-5 and C3G-6.

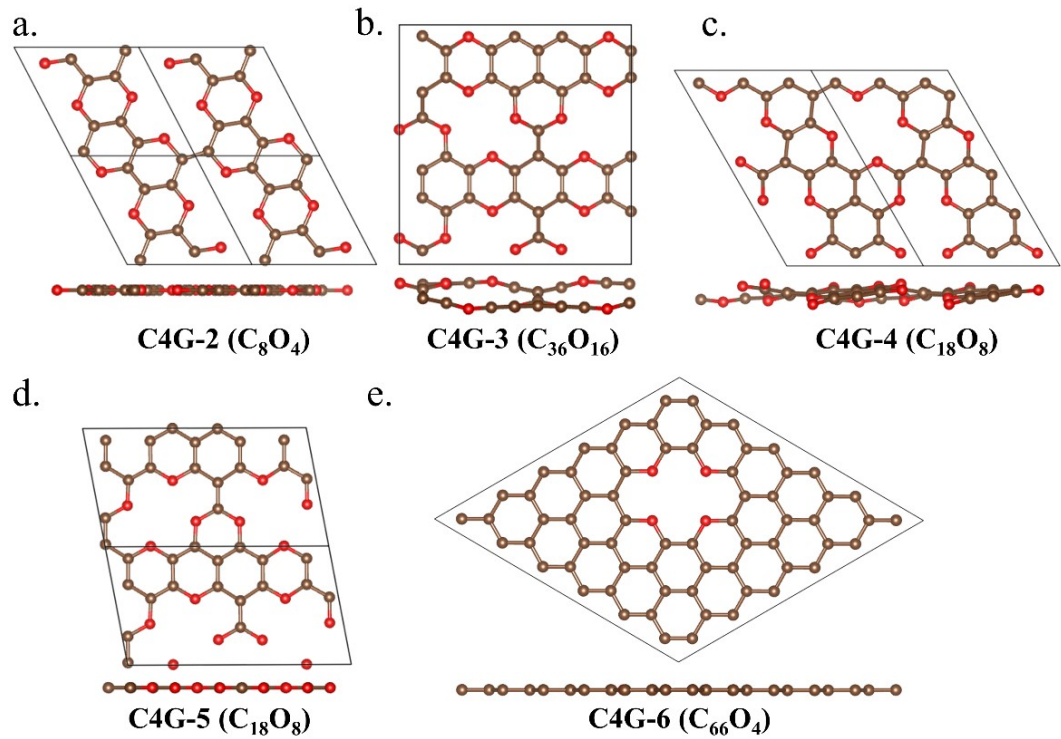


Figure S2. Top and side views of the optimized structures of (a) C4G-2, (b) C4G-3, (c) C4G-4, (d) C4G-5 and C4G-6.

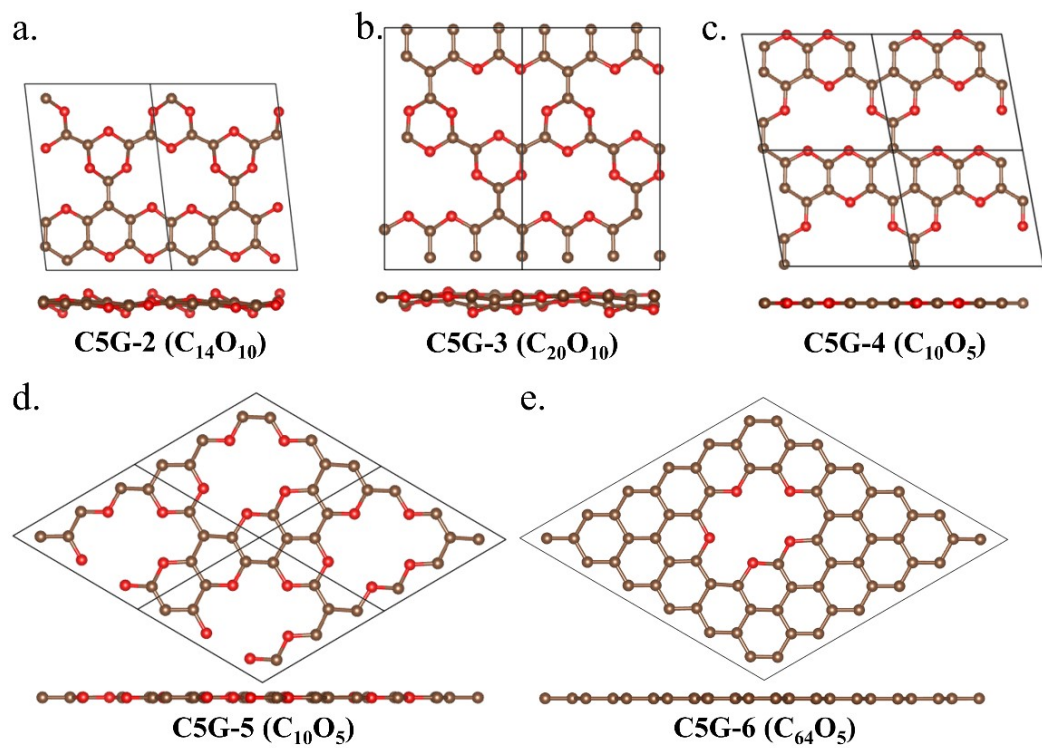


Figure S3. Top and side views of the optimized structures of (a) C5G-2, (b) C5G-3, (c) C5G-4, (d) C5G-5 and C5G-6.

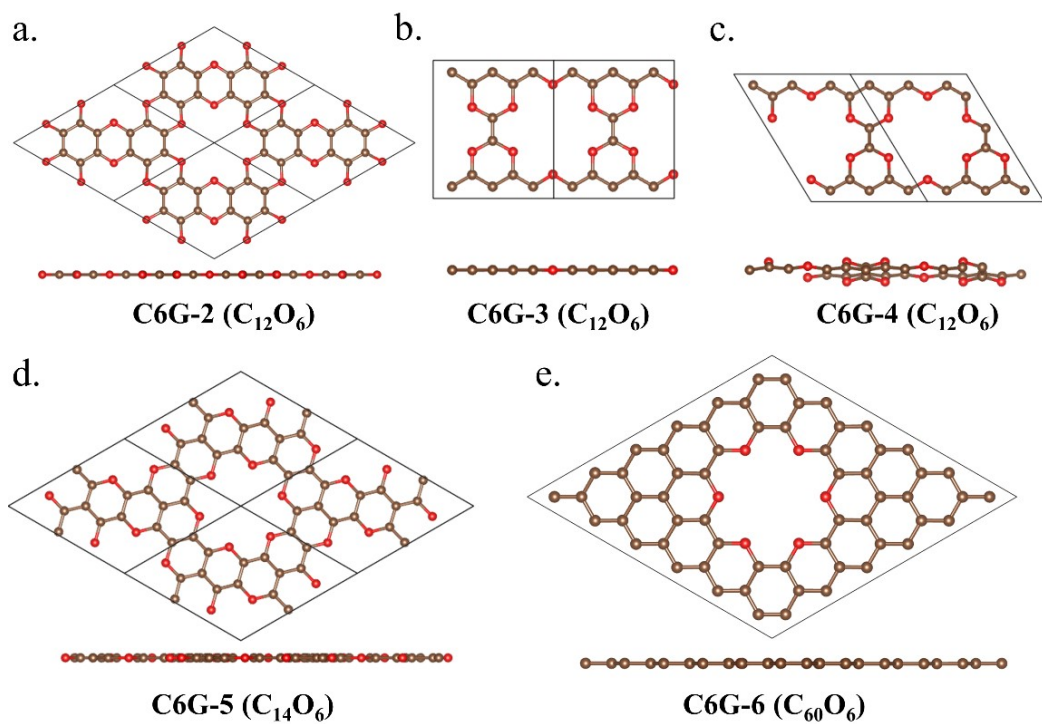


Figure S4. Top and side views of the optimized structures of (a) C6G-2, (b) C6G-3, (c) C6G-4, (d) C6G-5 and C6G-6.

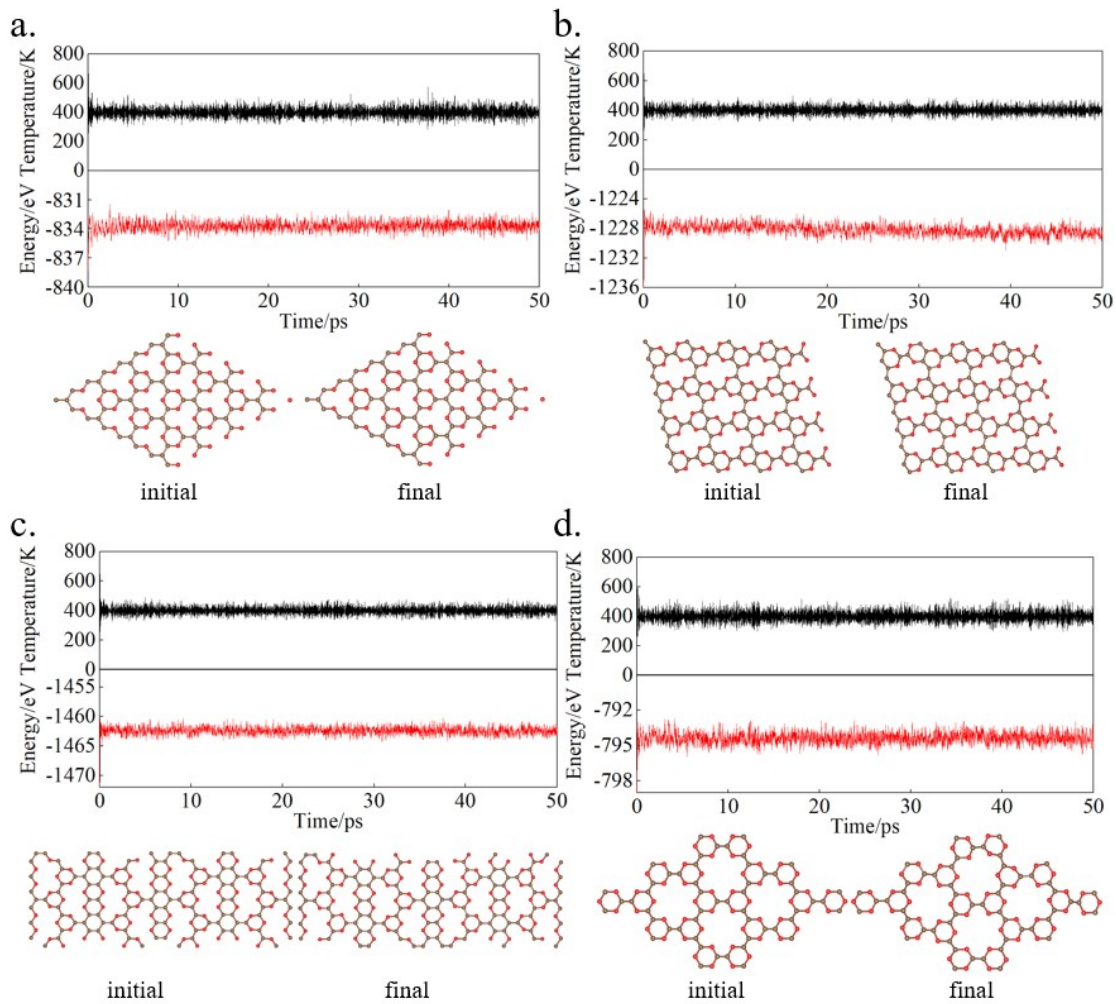


Figure S5. Fluctuation of temperature and energy against time for AIMD simulations at 400K: (a) C3G-1, (b) C4G-1, (c) C5G-1, (d) C6G-1. The initial and final snapshots of the simulations are also shown.

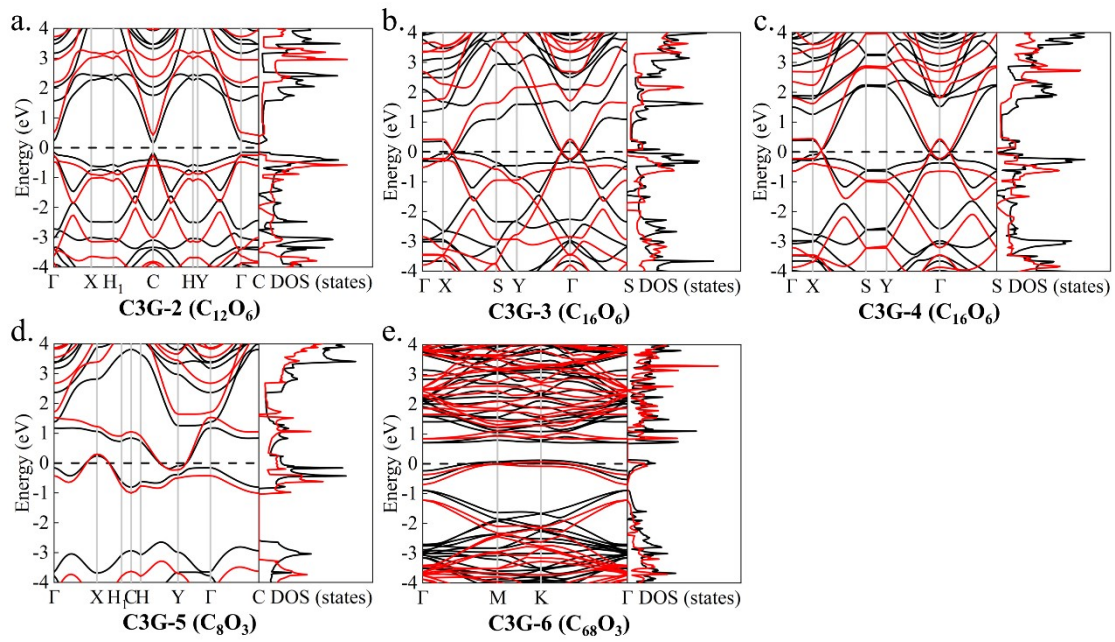


Figure S6. The band structures and DOS of (a) C3G-2, (b) C3G-3, (c) C3G-4, (d) C3G-5 and (e) C3G-6.

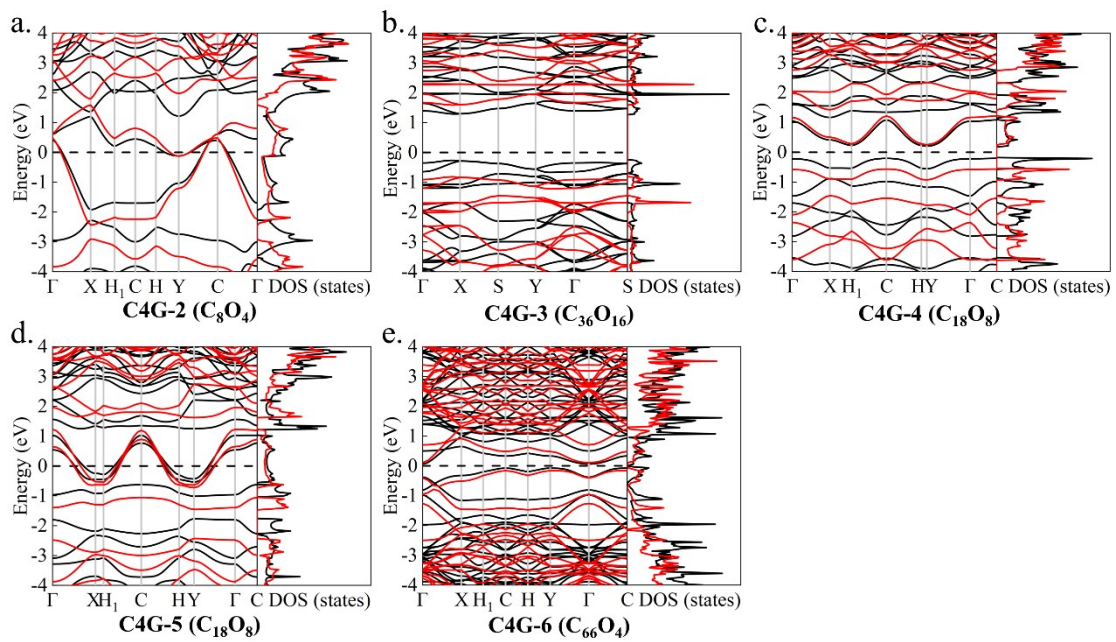


Figure S7. The band structures and DOS of (a) C4G-2, (b) C4G-3, (c) C4G-4, (d) C4G-5 and (e) C4G-6.

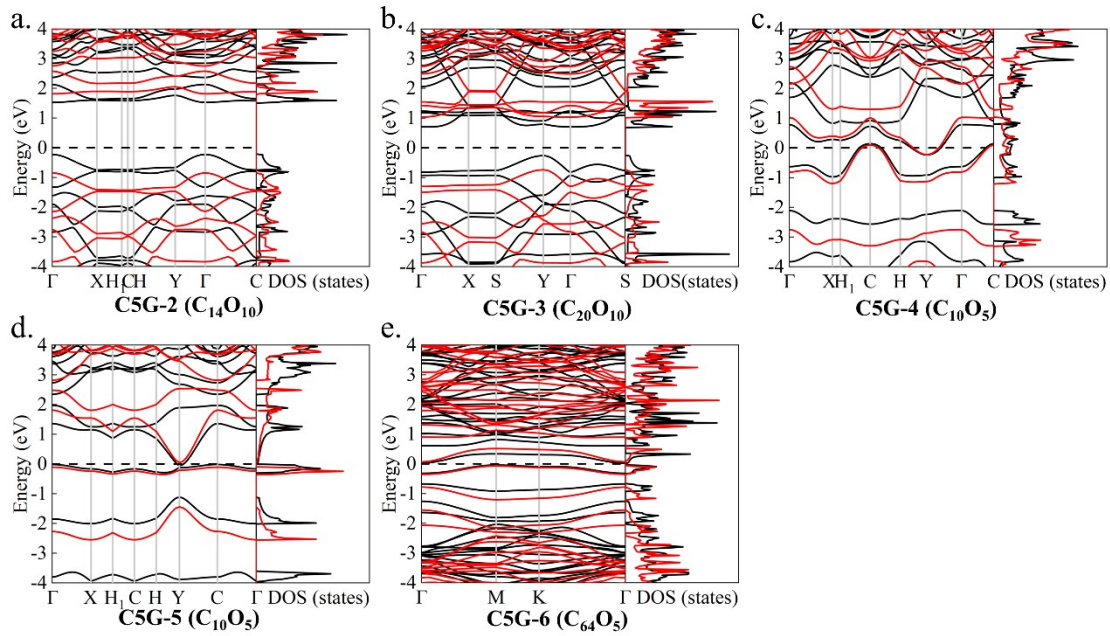


Figure S8. The band structures and DOS of (a) C5G-2, (b) C5G-3, (c) C5G-4, (d) C5G-5 and (e) C5G-6.

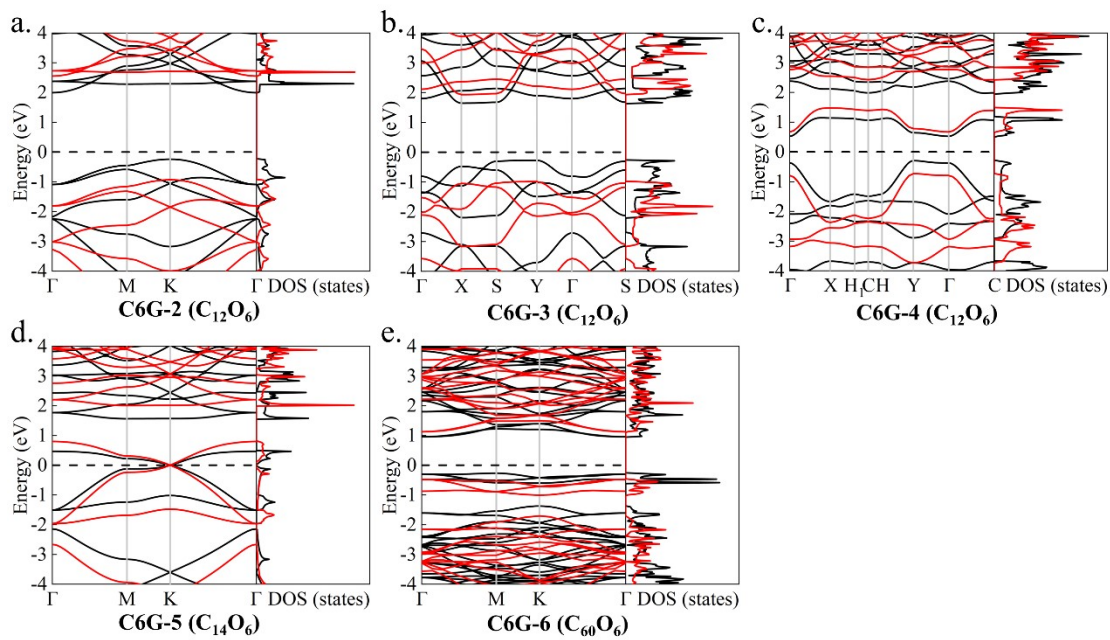


Figure S9. The band structures and DOS of (a) C6G-2, (b) C6G-3, (c) C6G-4, (d) C6G-5 and (e) C6G-6.

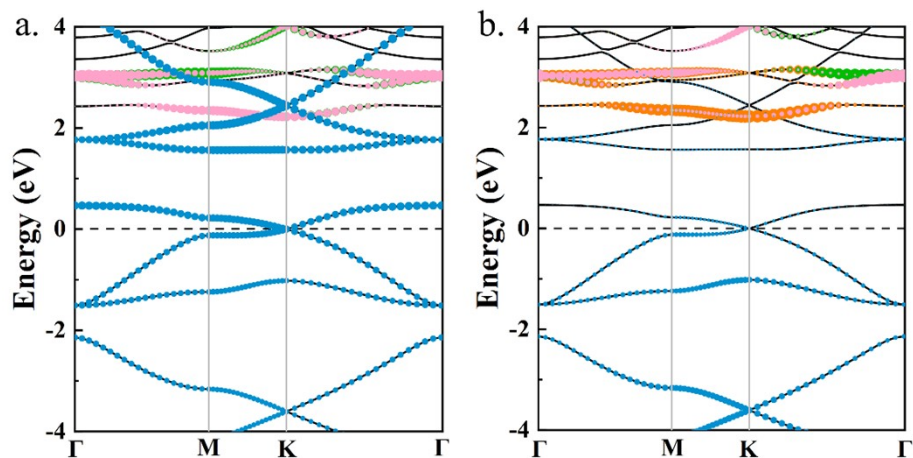


Figure S10. Orbital-projected band structures of (a) C atoms and (b) O atoms in C₆G-5. The orange, green, pink and blue points represent the s, p_x, p_y and p_z orbitals of C/O, respectively.

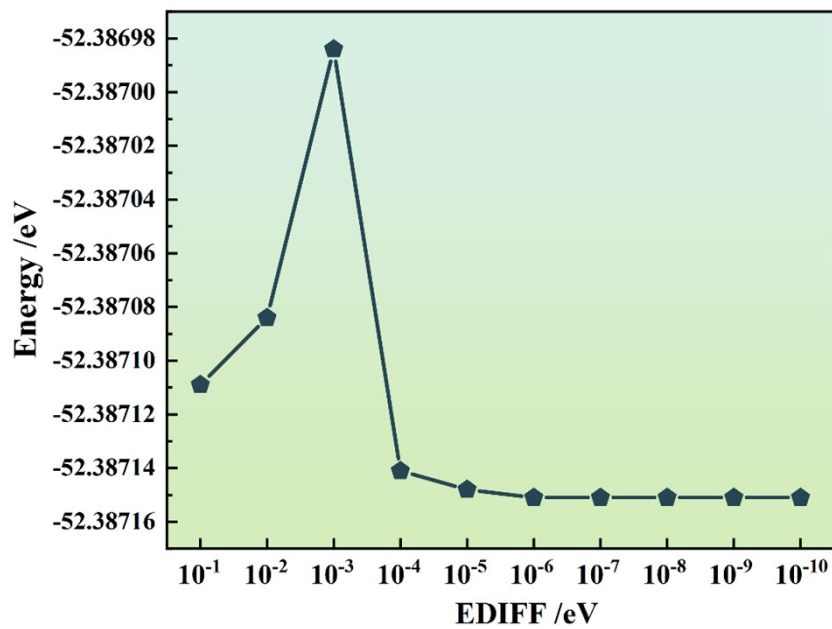


Figure S11. A diagram of the energy convergence standard test.